

Advanced Control Strategies for DC–DC Buck Converters With Parametric Uncertainties via Experimental Evaluation

Yunfei Yin¹, *Graduate Student Member, IEEE*, Jianxing Liu¹, *Senior Member, IEEE*,
 Abraham Marquez², *Member, IEEE*, Xinpo Lin, José I. Leon², *Fellow, IEEE*,
 Sergio Vazquez², *Senior Member, IEEE*, Leopoldo G. Franquelo², *Life Fellow, IEEE*,
 and Ligang Wu¹, *Fellow, IEEE*

Abstract—In this paper, four control strategies for DC-DC buck converters are proposed, compared and analyzed: a single-loop adaptive control strategy (SA), a double-loop adaptive control strategy (DA), a single-loop disturbance observer-based control strategy (SDOB) and a double-loop disturbance observer-based control strategy (DDOB). First, the nominal system without considering the parametric uncertainties of the DC-DC buck converter is built to help develop the SA and DA. The SA is built by adaptive and backstepping control approaches, and the DA is set up by adaptive and sliding mode control approaches. Additionally, a model considering parametric uncertainties is introduced, giving the opportunity to develop the SDOB and DDOB. The SDOB is developed using a designed disturbance observer and backstepping control technique, and the DDOB is synthesized using a designed disturbance observer and sliding mode control method. Finally, the advantages and disadvantages of the four proposed control strategies are compared and analyzed through experiments.

Index Terms—DC-dc buck converters, adaptive control, sliding mode control, disturbance observer.

I. INTRODUCTION

DC-DC converters are broadly used to achieve power conversion in a large variety of applications, such as hybrid electric vehicles, electrical equipment in medical systems,

portable recharging systems and power supplies. However, it is important to note that different application scenarios present specific requirements for the output voltage of the DC-DC converter [1]–[3]. For instance, some applications require DC-DC converters with a fast dynamic response and/or a small ripple in the output voltage. Other applications require a stable output voltage in the presence of load variations and parametric uncertainties. The comprehensive design of the most effective control strategy for every specific application has been the focus of industry and academia in recent decades [4]–[6].

Typically, there are two kinds of control structures, as shown in Fig. 1, i.e., single-loop and double-loop structures to control the DC-DC buck converter [7], [8]. Compared with the double-loop control strategy, the single-loop does not need to measure the current, leading to simple implementations in practice. Thus, the single-loop control is also called direct output control or voltage-mode control. The double-loop control structure consists of a voltage regulation loop and a current tracking loop. This approach is also called indirect output control. Since the double-loop control structure adopts the intermediate measured signal to quickly respond to the control requirements, it can provide tighter control and improve the system dynamic performance. Moreover, the double-loop control structure has a strong anti-interference ability because it allows the internal loop to control disturbances before affecting the primary control objective. Note that the process dynamics of the current tracking loop must act much faster than the dynamics of the voltage regulation loop [9].

Based on single-loop and double-loop control structures, numerous control strategies have been proposed to control DC-DC power converters in the past few decades [10]–[15]. First, based on the linear modeling, some linear control strategies were designed to control the buck converters [4]. However, it has been demonstrated that, the traditional linear controllers have worse dynamic performance than with nonlinear control schemes, [16]. In this way, various nonlinear control algorithms have been applied to DC-DC buck converters. To name a few, based on the single-loop control structure, a traditional sliding mode control (SMC) scheme was designed in [17]; a second-order sliding-mode (SOSM) controller was applied to DC-DC buck converters to regulate

Manuscript received January 19, 2020; revised April 14, 2020 and June 28, 2020; accepted July 9, 2020. This work was supported in part by the State Grid Heilongjiang Electric Power Company Limited funded project under Grant 522417190057, in part by the National Key Research and Development Program of China under Grant 2019YFB1312001, in part by the National Science Foundation of China under Grant 61525303, Grant 41772377, and Grant 61673130, in part the Self-Planned Task of State Key Laboratory of Advanced Welding and Joining (HIT) and in part by the Self-Planned Task of the State Key Laboratory of Robotics and System (HIT) under Grant SKLRS201806B. This article was recommended by Associate Editor E. Tlelo-Cuautle. (*Corresponding author: Ligang Wu.*)

Yunfei Yin, Jianxing Liu, Xinpo Lin, and Ligang Wu are with the Department of Control Science and Engineering, Harbin Institute of Technology, Harbin 150001, China (e-mail: ligangwu@hit.edu.cn).

Abraham Marquez, José I. Leon, and Sergio Vazquez are with the Electronic Engineering Department, Universidad de Sevilla, 41092 Sevilla, Spain.

Leopoldo G. Franquelo is with the Electronic Engineering Department, Universidad de Sevilla, 41092 Sevilla, Spain, and also with the Department of Control Science and Engineering, Harbin Institute of Technology, Harbin 150001, China.

Color versions of one or more of the figures in this article are available online at <http://ieeexplore.ieee.org>.

Digital Object Identifier 10.1109/TCSI.2020.3009168

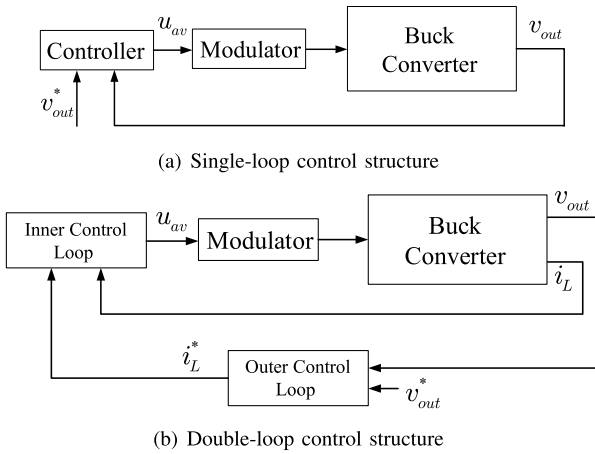


Fig. 1. Control structures for DC-DC buck converters.

the output voltage in [13], [18], [19]; in [20], based on the double-loop control structure, SOSM controllers were designed in the voltage regulation loop and current tracking loop, respectively; in [21]–[23], adaptive control technology was implemented in the converters; [24] constructed a fuzzy logic controller for dc–dc converters. Although these nonlinear control methods can improve the performance of the converter, most of the reported works assume that the nominal values of the filter inductor and output capacitor are the same as their actual values. However, there inevitably exist parametric uncertainties of the filter inductor and output capacitor in practice, which affect the control performance of the converter system. Moreover, some control strategies are highly nonlinear and complicated and have many control parameters, such as SOSM and intelligent control algorithms. Thus, they are difficult to analyze, design and implement. In addition, some control strategies are designed based on a single-loop control structure, and some are based on a double-loop control structure. Nevertheless, few works present an evaluation of the performance differences between these two classes of control structures through experiments.

To this end, four control strategies, a single-loop adaptive control strategy (SA), a double-loop adaptive control strategy (DA), a single-loop disturbance observer-based control strategy (SDOB) and a double-loop disturbance observer-based control strategy (DDOB), to regulate the output voltage of a DC-DC buck converter are proposed, compared and analyzed in this paper. The main contributions of this paper are as follows. First, to design the control strategies, the models of the system without and with parametric uncertainties of the DC-DC buck converter are reformulated. Then, based on these models, the SA, DA, SDOB and DDOB are designed. The SA is designed using an adaptive and backstepping control approach, which is the simplest structure among the four proposed control strategies. The DA applies an adaptive controller in the external loop, and the SMC is utilized in the internal loop. SA and DA have fewer control parameters and simpler control structure than the existing control strategies, which make them easier to design and implement in practice. The SDOB is built via a backstepping technique combined with a disturbance observer designed to estimate the

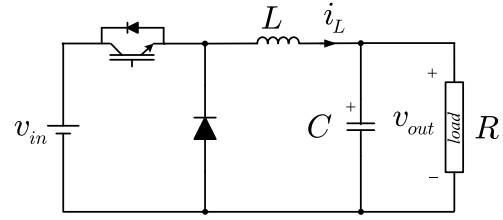


Fig. 2. DC-DC buck converter under study.

parametric uncertainties and unknown disturbances. Finally, for the DDOB, a disturbance observer-based controller is applied in the external loop to regulate the output voltage and an SMC plus a disturbance observer is utilized in the internal loop to force the inductor current tracking its reference. Compared with other works, a disturbance observer is constructed in SDOB and DDOB to estimate parametric uncertainties and disturbances, which can expand the application scope of control strategies.

The rest of the paper is organized as follows. In section II, the nominal and uncertain systems of the DC-DC buck converter and the control objectives are presented. The SA, DA, SDOB and DDOB control strategies are designed in sections III and IV, respectively. The main noticeable features of the four control strategies are discussed in section V. To compare and analyze the effectiveness of the four proposed control strategies, experimental results are given in section VI. Concluding remarks are summarized in section VII.

II. DC-DC BUCK CONVERTER MODEL

The circuit diagram of a DC-DC buck converter is depicted in Fig. 2, where v_{in} is the input voltage, L is the filter inductor, C is the output capacitor and R is the equivalent load considered the unknown disturbance. The averaged model of the buck converter in continuous conduction mode can be given as [17],

$$\dot{x}_1 = \frac{x_2}{C} - \frac{x_1}{RC}, \quad (1)$$

$$\dot{x}_2 = -\frac{x_1}{L} + \frac{v_{in}}{L}u_{av}, \quad (2)$$

where x_1 is the output voltage v_{out} , x_2 is the current through the inductor i_L and u_{av} is the control input. It should be noted that a study of the discontinuous conduction mode is not included in this paper for the sake of simplicity. The above system (1)-(2) is the nominal system for the converter without considering the parametric uncertainties of the filter inductor and output capacitor. However, in some practical applications, accurate values of the inductor and capacitor are not known. Taking this fact into account, the actual inductor and capacitor values are defined as follows:

$$\bar{L} = L + \Delta L, \bar{C} = C + \Delta C, \quad (3)$$

where L and C are the nominal values of the filter inductor and output capacitor, respectively, and ΔL and ΔC are the parametric uncertainties of filter inductor and output capacitor, respectively, which are considered unknown values.

Then, the uncertain system of the DC-DC buck converter can be written as,

$$\dot{x}_1 = \frac{x_2}{C} - \frac{x_1}{RC}, \quad (4)$$

$$\dot{x}_2 = -\frac{x_1}{L} + \frac{v_{in}}{L}u_{av}. \quad (5)$$

The dynamics of converters (4) and (5) can be rewritten as

$$\dot{x}_1 = \frac{x_2}{C} + d_1, \quad (6)$$

$$\dot{x}_2 = -\frac{x_1}{L} + \frac{v_{in}}{L}u_{av} + d_2, \quad (7)$$

where

$$d_1 = -\frac{\Delta C x_2}{C(C + \Delta C)} - \frac{x_1}{R(C + \Delta C)},$$

$$d_2 = \frac{\Delta L x_1}{L(L + \Delta L)} - \frac{\Delta L v_{in} u_{av}}{L(L + \Delta L)}.$$

Furthermore, the dynamics of converters (6) and (7) can be expressed as,

$$\dot{x} = Ax + Bu_{av} + d, \quad (8)$$

where $x = [x_1, x_2]^T$ and

$$A = \begin{bmatrix} 0 & \frac{1}{C} \\ -\frac{1}{L} & 0 \end{bmatrix}, B = \begin{bmatrix} 0 \\ \frac{v_{in}}{L} \end{bmatrix}, d = \begin{bmatrix} d_1 \\ d_2 \end{bmatrix}.$$

The objective of this paper is to regulate the output voltage to its desired reference in the presence of unknown disturbances and parametric uncertainties.

In the following section, based on the above dynamic models four control strategies will be designed to achieve the control objective. Before proceeding, the following lemma is presented.

Lemma 1: [25] *If $F \in \mathbb{R}^{n \times n}$ is the Hurwitz matrix, then there exists a positive scalar ϵ , such that $\|e^{Ft}\| \leq \epsilon e^{\frac{\lambda_{\max}}{2}t}$, where λ_{\max} is the largest eigenvalue of F .*

III. CONTROL STRATEGIES DESIGN FOR NOMINAL SYSTEM

In this section, based on the nominal system (1)-(2) the SA and DA controllers will be designed to achieve the control target. Next, the detailed design procedures will be given.

A. Single-Loop Adaptive Control Strategy

The voltage tracking error can be defined as

$$z_1 = x_1 - x_1^*, \quad (9)$$

where x_1^* is the desired output voltage. Taking the derivative of (9) along with (1), one can obtain

$$\dot{z}_1 = \frac{x_2}{C} - \theta x_1 - \dot{x}_1^*, \quad (10)$$

where $\theta = \frac{1}{RC}$ is the unknown parameter. Here it is assumed that the equivalent load R is unknown and changes in steps [13]. Thus θ is also unknown and changes in steps. Defining $\tilde{\theta} = \hat{\theta} - \theta$, one can construct the following Lyapunov function for the system (10), where $\hat{\theta}$ is the adaptive law to be designed,

$$V_{s11} = \frac{1}{2}z_1^2 + \frac{1}{2\eta}\tilde{\theta}^2. \quad (11)$$

Then, the time derivative of (11) is

$$\dot{V}_{s11} = z_1\left(\frac{x_2}{C} - \theta x_1 - \dot{x}_1^*\right) + \frac{1}{\eta}\tilde{\theta}\dot{\tilde{\theta}}. \quad (12)$$

Based on (12), one can design the virtual control α_1 , error variable z_2 and adaptive law $\tilde{\theta}$ as follows:

$$\alpha_1 = -k_{s11}z_1 + \dot{x}_1^* + \hat{\theta}x_1, \quad (13)$$

$$z_2 = \frac{x_2}{C} - \alpha_1, \quad (14)$$

$$\dot{\tilde{\theta}} = -\eta z_1 x_1, \quad (15)$$

where k_{s11} and η are positive scalars. Then, substituting (13)-(15) into (12) yields

$$\begin{aligned} \dot{V}_{s11} &= z_1(z_2 + \alpha_1 - \theta x_1 - \dot{x}_1^*) + \frac{1}{\eta}\tilde{\theta}\dot{\tilde{\theta}} \\ &= z_1(-k_{s11}z_1 + \hat{\theta}x_1 + z_2 + \dot{x}_1^* - \theta x_1 - \dot{x}_1^*) + \frac{1}{\eta}\tilde{\theta}\dot{\tilde{\theta}} \\ &= -k_{s11}z_1^2 + z_1z_2 + \tilde{\theta}z_1x_1 + \frac{1}{\eta}\tilde{\theta}(-\eta z_1x_1) \\ &= -k_{s11}z_1^2 + z_1z_2. \end{aligned} \quad (16)$$

Next, using (14), one can obtain the dynamic of z_2 ,

$$\dot{z}_2 = -\frac{x_1}{LC} + \frac{v_{in}}{LC}u_{av} - \dot{\alpha}_1. \quad (17)$$

The following Lyapunov function V_{s12} for the error system $z = [z_1, z_2]^T$ can be constructed:

$$V_{s12} = V_{s11} + \frac{1}{2}z_2^2. \quad (18)$$

Differentiating (18) yields

$$\begin{aligned} \dot{V}_{s12} &= -k_{s11}z_1^2 + z_1z_2 + z_2\dot{z}_2 \\ &= -k_{s11}z_1^2 + z_2\left(z_1 - \frac{x_1}{LC} + \frac{v_{in}}{LC}u_{av} - \dot{\alpha}_1\right). \end{aligned} \quad (19)$$

The control u_{av} which is designed so that $\dot{V}_{s12} < 0$ is satisfied, is given by

$$u_{av} = \frac{LC}{v_{in}}\left(-z_1 + \frac{x_1}{LC} + \dot{\alpha}_1 - k_{s12}z_2\right). \quad (20)$$

By substituting (20) into (19), it can be obtained that

$$\dot{V}_{s12} = -k_{s11}z_1^2 - k_{s12}z_2^2 \leq 0, \quad (21)$$

which means that the error system (z_1, z_2) tends to zero, i.e., the controller (20) can regulate the output voltage to its desired reference. Here, it should be noted that the way in which adaptive control technology is used in this paper is different from that used in [26], where the adaptive laws are designed using a state observer. The control structure of the SA is shown in Fig. 3.

B. Double-Loop Adaptive Control Strategy

1) *External Loop:* The aims of the external loop are to regulate the output voltage and provide the current command for the internal loop. It is assumed that the dynamics of the inner loop are faster than those of the outer loop; then, in line

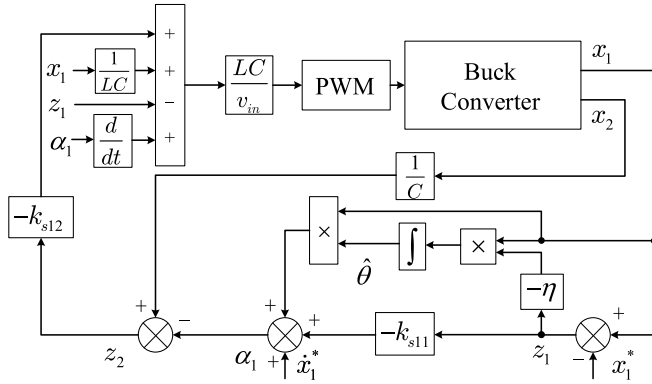


Fig. 3. The control structure of the SA.

with the singular perturbation theory [27], the dynamics of z_1 can be obtained as:

$$\dot{z}_1 = \frac{x_2^*}{C} - \theta x_1 - \dot{x}_1^*, \quad (22)$$

where x_2^* is the reference of x_2 . To achieve the control objective, the same Lyapunov function can be constructed as per (11). Then the reference of x_2 is designed as,

$$x_2^* = C(-k_{d1}z_1 + \dot{x}_1^* + \hat{\theta}x_1), \quad (23)$$

where k_{d1} is a positive scalar and the same adaptive law as per (15) is used.

2) *Internal Loop*: A sliding mode controller is employed in the internal loop to drive the inductor current to its reference provided from the external loop. From (2) one obtains the following derivative with $\tilde{x}_2 = x_2 - x_2^*$,

$$\dot{\tilde{x}}_2 = -\frac{x_1}{L} + \frac{v_{in}}{L}u_{av} - \dot{x}_2^*, \quad (24)$$

where \dot{x}_2^* satisfies the condition that $\|\dot{x}_2^*\|$ is less than or equal to the positive constant Φ . Next, the sliding mode controller u_{av} will be designed to drive the state trajectories onto the sliding surface \tilde{x}_2 in finite time. The Lyapunov function is constructed as

$$V_{d12} = \frac{1}{2}\tilde{x}_2^2. \quad (25)$$

The following derivative can be obtained by using (24),

$$\dot{V}_{d12} = \tilde{x}_2\left(-\frac{x_1}{L} + \frac{v_{in}}{L}u_{av} - \dot{x}_2^*\right). \quad (26)$$

One can design the following sliding mode controller:

$$u_{av} = -\frac{L}{v_{in}}(c_{d12}\tilde{x}_2 + D_{d12}\text{sign}(\tilde{x}_2) - \frac{x_1}{L}), \quad (27)$$

where c_{d12} and $D_{d12} \geq \Phi$ are positive constants. Applying the controller (27) in (26) yields

$$\begin{aligned} \dot{V}_{d12} &= \tilde{x}_2(-c_{d12}\tilde{x}_2 - D_{d12}\text{sign}(\tilde{x}_2) - \dot{x}_2^*) \\ &\leq -c_{d12}\tilde{x}_2^2 - D_{d12}|\tilde{x}_2| - \Phi\tilde{x}_2 \leq 0. \end{aligned} \quad (28)$$

Thus the inductor current x_2 can track its reference x_2^* in finite time. The control structure of the DA is shown in Fig. 4.

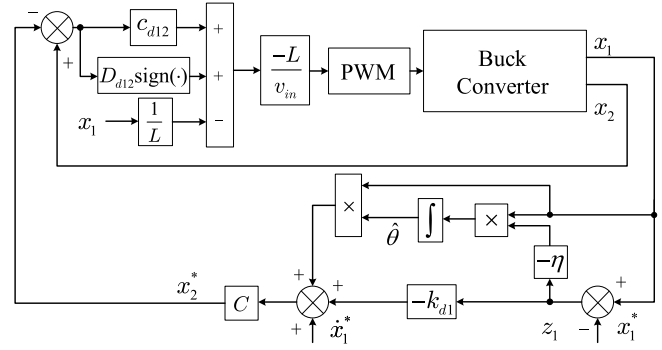


Fig. 4. The control structure of the DA.

IV. CONTROL STRATEGIES DESIGN FOR AN UNCERTAIN SYSTEM

In this section, the SDOB and DDOB controllers are applied to regulate the output voltage for an uncertain system in the presence of model parameter uncertainties and disturbances, respectively. The parametric uncertainties and unknown disturbances will be estimated by the disturbance observer.

A. Disturbance Observer Design

The disturbance observer that can estimate the disturbance d is presented as follows [28]:

$$\begin{aligned} \dot{\hat{d}} &= \zeta - Fx, \\ \dot{\zeta} &= F(Ax + Bu_{av} + \hat{d}), \end{aligned} \quad (29)$$

where $\hat{d} = [\hat{d}_1, \hat{d}_2]^T$ is the estimate vector of d , $\zeta = [\zeta_1, \zeta_2]^T$ is the internal state vector of the observer and

$$F = \begin{bmatrix} -f_{11} & 0 \\ 0 & -f_{22} \end{bmatrix},$$

with positive constants f_{11} and f_{22} to be designed, which means that F is the Hurwitz matrix. It can be derived from (8) and (29) that

$$\begin{aligned} \dot{\tilde{d}} &= \dot{\zeta} - F\dot{x} \\ &= F(Ax + Bu_{av} + \hat{d}) - F(Ax + Bu_{av} + d) \\ &= -F\tilde{d}, \end{aligned} \quad (30)$$

where $\tilde{d} = d - \hat{d}$ is the estimated error vector.

Using (30), the following derivative can be obtained following derivative,

$$\dot{\tilde{d}} = \dot{d} + F\tilde{d}, \quad (31)$$

and its solution can be written as

$$\tilde{d} = e^{Ft}\tilde{d}_0 + \int_0^t e^{F(t-\tau)}\dot{d}(\tau)d\tau, \quad (32)$$

where \tilde{d}_0 is the initial value of \tilde{d} . Assuming that $\|d\| \leq \phi$ and $\|\dot{d}\| \leq \varsigma$, according to Lemma 1, one can obtain

$$\begin{aligned} \|\tilde{d}\| &= \|e^{Ft}d_0\| + \left\| \int_0^t e^{F(t-\tau)}\dot{d}(\tau)d\tau \right\| \\ &\leq \|e^{Ft}\| \|d_0\| + \int_0^t \|e^{F(t-\tau)}\| \|\dot{d}(\tau)\| d\tau \end{aligned}$$

$$\begin{aligned} &\leq \epsilon\phi e^{\frac{\lambda_{\max}(F)}{2}t} + \epsilon\varsigma \frac{2}{\lambda_{\max}(F)}(e^{\frac{\lambda_{\max}(F)}{2}t} - 1) \\ &\leq \epsilon\phi - \epsilon\varsigma \frac{2}{\lambda_{\max}(F)}. \end{aligned} \quad (33)$$

Therefore, it can be concluded that estimate errors are ultimately bounded.

B. Single-Loop Disturbance Observer-Based Control Strategy

Taking the derivative of (9) along with (6), one can obtain

$$\dot{z}_1 = \frac{x_2}{C} + d_1 - \dot{x}_1^*. \quad (34)$$

The following Lyapunov function is constructed for the system (34),

$$V_{s21} = \frac{1}{2}z_1^2. \quad (35)$$

Then, the time derivative of (35) is

$$\dot{V}_{s21} = z_1\left(\frac{x_2}{C} + d_1 - \dot{x}_1^*\right). \quad (36)$$

Based on (36), one can design the virtual control α_2 and the error variable z_2 as follows:

$$\alpha_2 = -k_{s21}z_1 + \dot{x}_1^* - \hat{d}_1, \quad (37)$$

$$z_2 = \frac{x_2}{C} - \alpha_2, \quad (38)$$

where k_{s21} is a positive scalar. Then, (36) becomes

$$\begin{aligned} \dot{V}_{s21} &= z_1(-k_{s21}z_1 + \dot{x}_1^* - \hat{d}_1 + d_1 - \dot{x}_1^* + z_2) \\ &= -k_{s21}z_1^2 + z_1z_2 + z_1\tilde{d}_1. \end{aligned} \quad (39)$$

The time derivative of z_2 can be obtained from (7) and (38),

$$\dot{z}_2 = -\frac{x_1}{LC} + \frac{v_{in}}{LC}u_{av} + \frac{d_2}{C} - \dot{\alpha}_2. \quad (40)$$

It is natural to construct the following Lyapunov function,

$$V_{s22} = V_{s21} + \frac{1}{2}z_2^2. \quad (41)$$

Using (39) and (40), the following derivative can be obtained:

$$\begin{aligned} \dot{V}_{s22} &= -k_{s21}z_1^2 + z_1z_2 + z_1\tilde{d}_1 + z_2\dot{z}_2 \\ &= -k_{s11}z_1^2 + z_2\left(z_1 - \frac{x_1}{LC} + \frac{v_{in}}{LC}u_{av} + \frac{d_2}{C} - \dot{\alpha}_2\right) + z_1\tilde{d}_1. \end{aligned} \quad (42)$$

The control u_{av} is designed as

$$u_{av} = \frac{LC}{v_{in}}\left(-z_1 + \frac{x_1}{LC} + \dot{\alpha}_2 - k_{s22}z_2 - \frac{\hat{d}_2}{C}\right), \quad (43)$$

where k_{s22} is a positive scalar.

Then (42) becomes, substituting (43) into (42),

$$\begin{aligned} \dot{V}_{s22} &= -k_{s11}z_1^2 - k_{s22}z_2^2 + z_1\tilde{d}_1 + z_2\frac{\tilde{d}_2}{C}, \\ &= z^T \begin{bmatrix} -k_{s21} & 0 \\ 0 & -k_{s22} \end{bmatrix} z + z^T \tilde{d}', \end{aligned} \quad (44)$$

where $z = [z_1, z_2]^T$ and $\tilde{d}' = [\tilde{d}_1, \frac{\tilde{d}_2}{C}]^T$. Since the estimate error vector \tilde{d} is bounded, the vector \tilde{d}' is also bounded.

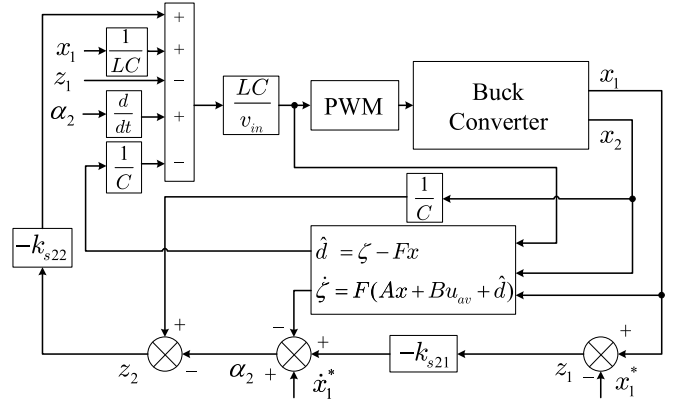


Fig. 5. The control structure of the SDOB.

Without loss of generality, assume that $\|\tilde{d}'\| \leq \varrho$. Moreover, it can be obtained that

$$\begin{aligned} \dot{V}_{s22} &\leq -z^T \begin{bmatrix} k_{s11} & 0 \\ 0 & k_{s22} \end{bmatrix} z + \|z^T\| \|\tilde{d}'\| \\ &\leq -\min\{k_{s11}, k_{s22}\} \|z\|^2 + \|z\| \varrho \\ &= -\|z\| (\min\{k_{s11}, k_{s22}\} \|z\| - \varrho). \end{aligned} \quad (45)$$

Thus, the ultimate bound of z is given by

$$\|z\| \leq \frac{\varrho}{\min\{k_{s11}, k_{s22}\}}. \quad (46)$$

The control structure of the SDOB is shown in Fig. 5.

C. Double-Loop Disturbance Observer-Based Control Strategy

1) *External Loop*: Using (6) and (9), the dynamic of the external loop can be rewritten as

$$\dot{z}_1 = \frac{x_2^*}{C} + d_1 - \dot{x}_1^*. \quad (47)$$

Based on the disturbance observer, the composite controller can be designed as

$$x_2^* = C(-k_{d2}z_1 + \dot{x}_1^* - \hat{d}_1), \quad (48)$$

where k_{d2} is a positive scalar and \hat{d}_1 is the estimated value of d_1 , which is similar to (29) and is omitted here.

Here, it should be pointed out that the disturbance observer used in the double-loop control structure is different from that used in the single-loop control structure. In the single-loop control structure, the disturbances d_1 and d_2 are estimated simultaneously, while the disturbances d_1 and d_2' which will be explained in the next subsection, are estimated in the external loop and internal loop respectively, in the double-loop control strategy.

Using (48), the dynamic of the external loop becomes

$$\dot{z}_1 = -k_{d2}z_1 + \tilde{d}_1, \quad (49)$$

and its solution is given as

$$z_1 = e^{-k_{d2}t} z_{10} + \int_0^t e^{-k_{d2}(t-\tau)} \tilde{d}_1(\tau) d\tau, \quad (50)$$

where z_{10} is the initial value of z_1 .

It can be concluded from (32), that z_1 is ultimately bounded.

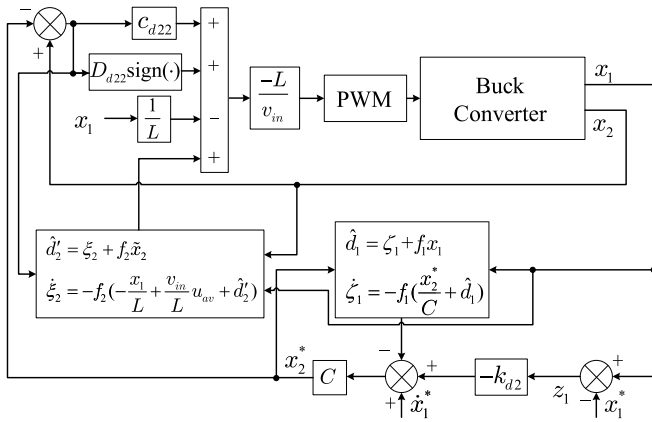


Fig. 6. The control structure of the DDOB.

2) *Internal Loop*: From (7) the error the dynamic of internal loop can be rewritten as,

$$\dot{\tilde{x}}_2 = -\frac{x_1}{L} + \frac{v_{in}}{L}u_{av} + d'_2, \quad (51)$$

where $d'_2 = d_2 - \dot{x}_2^*$. Here, the disturbance observer is still utilized to estimate the disturbance d'_2 . The disturbance observer can be designed as,

$$\begin{aligned} \dot{\hat{d}}'_2 &= \xi_2 + f_2 \tilde{x}_2, \\ \dot{\xi}_2 &= -f_2 \left(-\frac{x_1}{L} + \frac{v_{in}}{L}u_{av} + \hat{d}'_2 \right), \end{aligned} \quad (52)$$

where \hat{d}'_2 is the estimate of disturbance, d'_2 , f_2 is a positive constant and ξ_2 is the internal state vector of the observer. The process of stability and analysis of the disturbance observer is similar to that presented in section IV-A, and it is omitted here. The observation error $\tilde{d}'_2 = d'_2 - \hat{d}'_2$ satisfies $\|\tilde{d}'_2\| \leq \varpi$.

Next, one can take advantage of \hat{d}'_2 to design a sliding mode controller to force the inductor current towards its reference.

Based on the Lyapunov function (25), one can obtain its derivative from (51),

$$\dot{V}_{d22} = \tilde{x}_2 \left(-\frac{x_1}{L} + \frac{v_{in}}{L}u_{av} + d'_2 \right), \quad (53)$$

where $\tilde{x}_2 = x_2 - x_2^*$ is the sliding variable.

One can design the following sliding mode controller,

$$u_{av} = -\frac{L}{v_{in}}(c_{d22}\tilde{x}_2 + D_{d22}\text{sign}(\tilde{x}_2) - \frac{x_1}{L} + \hat{d}'_2), \quad (54)$$

where c_{d22} is a positive scalar and D_{d22} satisfies $D_{d22} \geq \varpi$. Then, using (54), the Lyapunov function derivative (53) becomes,

$$\begin{aligned} \dot{V}_{d22} &= \tilde{x}_2(-c_{d22}\tilde{x}_2 - D_{d22}\text{sign}(\tilde{x}_2) + \tilde{d}'_2) \\ &\leq -c_{d22}\tilde{x}_2^2 - D_{d22}|\tilde{x}_2| + \varpi\tilde{x}_2 \leq 0. \end{aligned} \quad (55)$$

This relation implies that the inductor current x_2 can track its reference x_2^* in finite time. The control structure of the DDOB is shown in Fig. 6.

Remark 1: Four control strategies have been proposed for the DC-DC buck converter. For the single-loop control strategies SA and SDOB, the stability of the closed-loop system under the controllers (20) and (43) have been strictly proven

in sections III. A and IV. B by the Lyapunov function methods. For the double-loop control strategies DB and DDOB, the stability of the closed-loop system have been proven in many works [7], [29]. On the other hand, it should be noted that the application background of this paper is focused on DC-DC buck converters. However, these control strategies also can be extended to the other converters, such as DC-DC boost converters and buck-boost converters.

V. DISCUSSION

In section III, the SA and DA controllers are designed to achieve the control target for the nominal system without considering parametric uncertainties. However, in some practical applications, the values of the inductor and capacitor of the DC-DC buck converter are not exact. Therefore, in section IV the SDOB and DDOB are implemented for an uncertain system in the presence of model uncertainties and disturbances to regulate the output voltage. Although the SA and SDOB are developed based on a single-loop control structure, it should be noted that the single-loop control structure of this paper is different from the conventional single-loop control structure that only uses the output voltage information, as shown in Fig. 1(a). The single-loop control structure proposed in this paper also adopts an intermediate variable to assist in achieving the primary control objective, which is similar to the double-loop control idea.

On the other hand, in section III, an efficient adaptive controller is designed in the single-loop control structure and voltage regulation loop of the double-loop control structure. In the voltage regulation loop, based on singular perturbation theory, variable x_2^* is viewed as the resulting control signal. However, in the single-loop control structure, x_2 is not viewed as the actual control input, and a new error variable z_2 is introduced to compensate for variable x_2 . Although the intermediate variable x_2 is used in both control structures, the way used are totally different. The former requires that the dynamic of x_2 must be much faster than that of x_1 . The latter does not have this requirement, and an error variable must be added.

In section IV, a disturbance observer is utilized to estimate the parametric uncertainties and disturbance for the uncertain system to improve system performance. Then, the disturbance observer is applied in the single-loop and double-loop control structures respectively to regulate the output voltage. Note that compared with section III, the voltage tracking error z_1 in the single-loop control structure cannot asymptotically reach zero since the disturbance observer cannot asymptotically estimate the unknown disturbance. However it is based on the concept of ultimate boundedness [30], which is also referred to as practical stability. For the double-loop control structure, a proportional controller coupled with a disturbance observer has been designed in the external loop which also cannot guarantee the asymptotic convergence of the voltage tracking error z_1 , but rather its ultimate boundedness. However, a sliding mode controller is implemented in the internal loop, which can force the inductor current to asymptotically track its reference, because the sliding mode controller is insensitive to parameter uncertainties and disturbances.

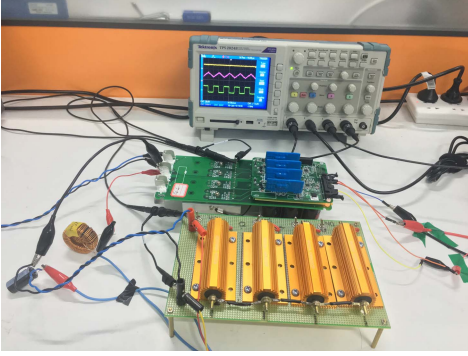


Fig. 7. Laboratory prototype of DC-DC buck converter.

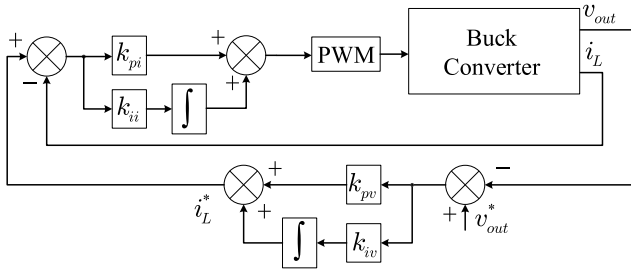


Fig. 8. The control structure of PI control strategy.

TABLE I
NOMINAL PARAMETERS OF THE BUCK CONVERTER

Description	Parameter	Nominal Value	Units
Switching frequency	f_{sw}	10	kHz
Inductor	L	$1.5 \cdot 10^{-3}$	H
Capacitor	C	$2.2 \cdot 10^{-3}$	F
Load resistance	R	$20 \rightarrow 10$	Ω
Input voltage	v_{in}	30	V
Reference voltage	x_1^*	$15 \rightarrow 12$	V

VI. EXPERIMENTAL RESULTS

In this section, experimental results are shown to compare and analyze the effectiveness of the four proposed strategies for DC-DC buck converters. The laboratory prototype of the DC-DC buck converter with the proposed controller is shown in Fig. 7. To better compare and analyze the four proposed controllers, a MATLAB/Simulink-compatible dSPACE 1202 platform is selected to drive the converter circuit. The nominal parameters of the buck converter and the control parameters of the proposed control strategies are presented in Table I and Table II, respectively. The control objective is to regulate the output voltage and experimental results are given in two cases: load resistance and reference voltage variations. To show the advantages of the proposed control strategies, a comparative experiment using the typical cascaded PI controller, whose control structure is shown in Fig. 8, is implemented as well.

A. Load Resistance Variations

In this experiment, the reference voltage is kept constant at 15 V, and the load resistance is changed from 20 Ω to

TABLE II
CONTROL PARAMETERS OF THE PROPOSED CONTROL STRATEGIES

Control Strategy	Control parameters	
SA	$\eta = 1200, k_{s11} = 150, k_{s12} = 200$	
DA	External Loop	$k_{d1} = 2.6, \eta = 120$
	Internal Loop	$c_{d1} = 500, D_{d12} = 0.05$
SDOB	$f_{11} = 300, f_{12} = 300, k_{s12} = 50, k_{s22} = 1500$	
DDOB	External Loop	$f_1 = 10, k_{d2} = 2.5$
	Internal Loop	$f_2 = 50, c_{d22} = 300, D_{d22} = 0.05$

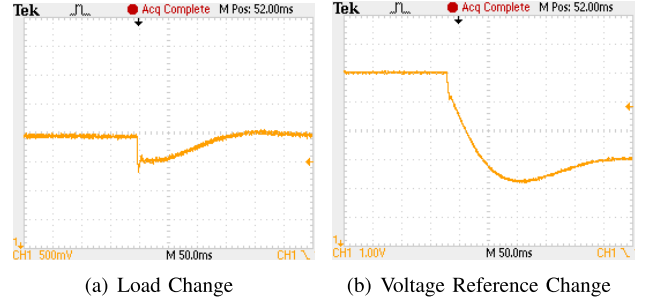


Fig. 9. Output voltage of the PI control strategy.

10 Ω . The dynamics of the output voltage of the PI and the four proposed control strategies measured by an oscilloscope are shown in the Figs. 9(a) and 10, respectively. It can be observed from Figs. 9(a) and 10 that all the control strategies can regulate the output voltage to its reference values of 15 V even under the load changes. The voltage drop and recovery time of all control strategies when the load changes are presented in Table III. As shown in the Figs. 9(a) and 10, compared with the four proposed control approaches, the PI control strategy needs the longest time to recover when the load changes. The SA has the shortest recovery time of 15 ms when the load changes. The DA presents less output voltage drop but longer dynamic response time than the SA. Note that among the four control strategies the DA has the smallest voltage drop when the load changes. The SDOB has slower dynamic response and a larger voltage drop than the SA and DA. In addition, among the proposed four control strategies, the DDOB needs the longest time to recover when the load changes. The static performances of the different control strategies are shown in Table IV. It can be observed that the DDOB exhibits the best static performances.

It is worth noting that both the SA and DA present smaller voltage drops than the SDOB and DDOB when the load changes. The reason is that SA and DA take advantage of adaptive law to adapt the unknown parameter $\theta = \frac{1}{RC}$; nevertheless, the SDOB and DDOB need to estimate the disturbance $d_1 = -\frac{\Delta C x_2}{C(C+\Delta C)} - \frac{x_1}{R(C+\Delta C)}$. Note that when the load changes, the change is only in R . The best way to regulate the output voltage is only to estimate R , rather than the total disturbance d_1 . From this point, the adaptive approach achieves a better performance than disturbance observer-based control approaches. On the other hand, it can be observed that the single-loop control structure has a shorter recovery time, but

TABLE III
THE DETAILED RESULTS OF THE CONTROL STRATEGIES
WHEN THE LOAD CHANGES

Control Strategy	Voltage Drop (mV)	Recovery Time (ms)
SA	650	15
DA	500	70
SDOB	750	65
DDOB	740	150
PI	700	160

TABLE IV
THE STATIC PERFORMANCE OF THE DIFFERENT CONTROL STRATEGIES

Control Strategy	Mean Error	Mean Square Error	Error Variance
SA	0.1450	0.1463	3.9224×10^{-4}
DA	0.2039	0.2045	2.4150×10^{-4}
SDOB	0.1575	0.1586	3.4301×10^{-4}
DDOB	0.1400	0.1412	3.3382×10^{-4}
PI	0.1661	0.1672	3.5580×10^{-4}

the double-loop control structure has a lower output voltage drop when the load changes. Specifically, for SA (SDOB) and DA (DDOB), the former has faster dynamic response, but the latter achieves a better output voltage drop performance. This finding means that the double-loop control structure has stronger robustness to disturbance than the single-loop control structure, but its dynamic response time is slower when the load changes.

Moreover, the following experiments are provided, where the model of the buck converter in the controller is changed, to further investigate the robustness of the proposed control strategies (SDOB and DDOB) to uncertain parameters. In the first experiment, the values of the inductor and capacitor are set to $\bar{L} = L + 20\%L$ and $\bar{C} = C + 20\%C$, respectively, and in the second experiment, the values of the inductor and capacitor are set to $\bar{L} = L - 20\%L$ and $\bar{C} = C - 20\%C$, respectively. It can be observed that the dynamics of the output voltage in Fig. 11 have the similar dynamics as those in Figs. 10(c) and 10(d), respectively, in which the inductor and capacitor use nominal values. The differences in the output voltage dynamics when increasing and decreasing the values of the inductor and capacitor are acceptable when using the SDOB and DDOB. This finding means that the SDOB and DDOB are robust to uncertainties in the model parameters.

B. Reference Voltage Variations

In this experiment, the reference voltage is changed from 15 V to 12 V, and the load resistance is 20 Ω . The control parameters remain unchanged. The dynamics of the output voltage of the PI and the four proposed control strategies measured by an oscilloscope are shown in Figs.9(b) and 12, respectively. The voltage undershoots and recovery times of all control strategies when the reference voltage changes are presented in Table V. It can be seen that all the control strategies

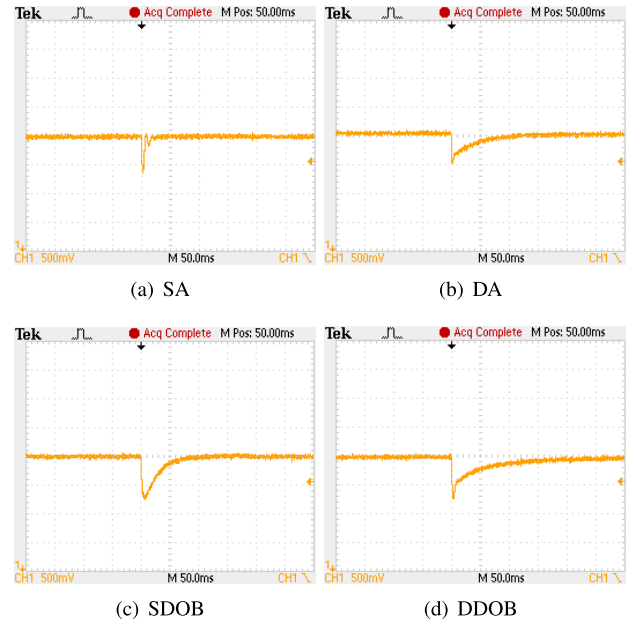


Fig. 10. Output voltage (500 mV/div) of the four control strategies when load changes.

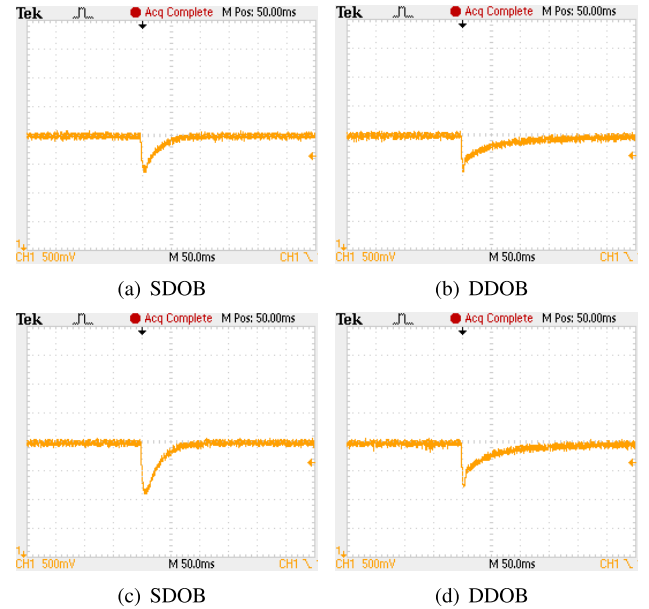


Fig. 11. Output voltages of the SDOB and DDOB under variations of inductor and capacitor, i.e., (a) +20% variations in the inductor and capacitor using SDOB, (b) +20% variations in the inductor and capacitor using DDOB, (c) -20% variations in the inductor and capacitor using SDOB, and (d) -20% variations in the inductor and capacitor using DDOB.

are robust to reference voltage variations and can regulate the output voltage to its new reference value. However, they exhibit different performances. Specifically, for PI control, the settling time of the output voltage is the longest, and the voltage undershoot is higher than that in the other control strategies except the SA. The SA still has the fastest recovery time, but its voltage undershoot is the highest among the four control strategies. The DA has lower voltage undershoot than the SA, but requires the longest time to recover when the

TABLE V
THE DYNAMIC PERFORMANCE OF THE CONTROL STRATEGIES
WHEN THE REFERENCE VOLTAGE CHANGES

Control Strategy	Voltage Undershoot (mV)	Recovery Time (ms)
SA	900	30
DA	400	120
SDOB	0	60
DDOB	600	80
PI	800	260

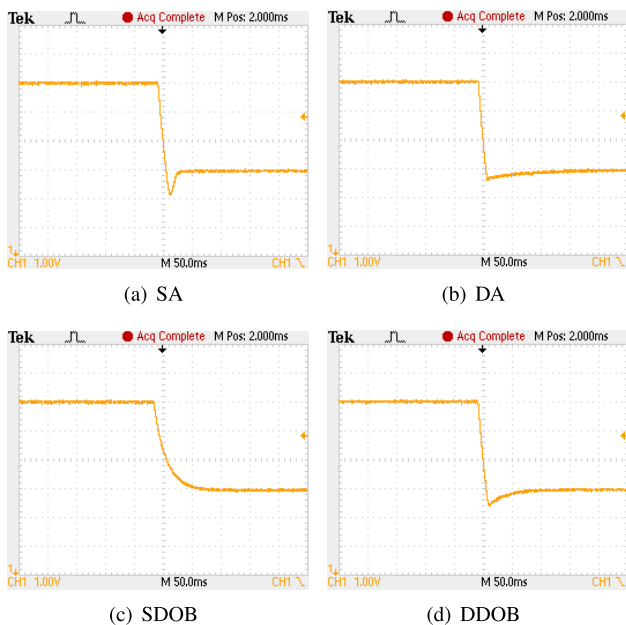


Fig. 12. Output voltages (1 V/div) of the four control strategies when the reference changes.

reference voltage changes. The SDOB does not have a voltage undershoot under reference voltage variations. The DDOB requires a longer recovery time than the SDOB.

Therefore, depending on individual application requirements, one can select or switch to the most effective control strategy for the DC-DC buck converter to achieve the best performance. For example, as some applications require DC-DC converters with fast dynamic responses when the load and reference voltage change, one can select or switch to the SA to meet these requirements.

VII. CONCLUSION

The problem of output voltage regulation in a DC-DC buck converter has been investigated in this paper. Based on the nominal and uncertain systems of the DC-DC buck converter, four control strategies (i.e., SA, DA, SDOB and DDOB) have been proposed. The characteristics and design procedures of the four control strategies are compared, discussed and analyzed. Two experimental results namely, the results of the comparison of the controller vs. the load resistance variations and the comparison of the controller vs. the reference voltage variations, are provided to further compare and analyze the

advantages and disadvantages of the four proposed strategies. The SA can ensure that the output voltage has the shortest recovery time whenever the load or the reference voltage changes. The output voltage has the smallest output voltage drop under a sudden load change using the DA. The SDOB is robust to reference voltage changes without an output voltage undershoot. The DDOB achieves the best static performance among the four proposed control strategies. From the present study and analysis, one can select or switch to the most suitable control strategy for any application scenario. In fact, none of the existing control strategies for DC-DC converters can be declared the “best”. Any selected control scheme should depend on the specific application requirements and balance the complexity of the control strategy, regulation quality of the output voltage and robustness. Further study will focus on the direct design of digital controllers such as discretized quasi-sliding mode controller for DC-DC buck converters. On the other hand, how to design an efficient controller for DC-DC buck converters consider the practical inductor and capacitor with parasitic resistances is still an open problem.

REFERENCES

- [1] M. K. Kazimierczuk, *Pulse-Width Modulated DC-DC Power Converters*. Hoboken, NJ, USA: Wiley, 2015.
- [2] E. Hernández-Márquez *et al.*, “Robust tracking controller for a DC/DC buck-boost converter–inverter–DC motor system,” *Energies*, vol. 11, no. 10, pp. 2500–2515, 2018.
- [3] J. I. Leon, S. Vazquez, and L. G. Franquelo, “Multilevel converters: Control and modulation techniques for their operation and industrial applications,” *Proc. IEEE*, vol. 105, no. 11, pp. 2066–2081, Nov. 2017.
- [4] H.-H. Park and G.-H. Cho, “A DC–DC converter for a fully integrated PID compensator with a single capacitor,” *IEEE Trans. Circuits Syst. II, Exp. Briefs*, vol. 61, no. 8, pp. 629–633, Aug. 2014.
- [5] S.-C. Tan, Y. M. Lai, M. K. H. Cheung, and C. K. Tse, “On the practical design of a sliding mode voltage controlled buck converter,” *IEEE Trans. Power Electron.*, vol. 20, no. 2, pp. 425–437, Mar. 2005.
- [6] E. Hernández-Márquez *et al.*, “New “full-bridge buck inverter–dc motor” system: Steady-state and dynamic analysis and experimental validation,” *Electron.*, vol. 8, no. 11, pp. 1216–1235, 2019.
- [7] S. Bacha *et al.*, *Power Electronic Converters Modeling and Control* (Advanced Textbooks in Control and Signal Processing). New York, NY, USA: Springer, 2014.
- [8] L. Dixon, “Average current mode control of switching power supplies,” in *Unitrode Power Supply Design Seminar Handbook*. Merrimack, NH, USA: Unitrode Corp., 1990.
- [9] K. J. Åström and T. Häggglund, *PID Controllers: Theory, Design, and Tuning*. Triangle Park, NC, USA: Instrument Society of America Research, 1995.
- [10] K. Hyeon Kim, J. Kim, H. Jun Kim, S. Hee Han, and H. Jung Kim, “A megahertz switching DC/DC converter using FeBN thin film inductor,” *IEEE Trans. Magn.*, vol. 38, no. 5, pp. 3162–3164, Sep. 2002.
- [11] J. Sha, D. Xu, Y. Chen, J. Xu, and B. W. Williams, “A peak-capacitor-current pulse-train-controlled buck converter with fast transient response and a wide load range,” *IEEE Trans. Ind. Electron.*, vol. 63, no. 3, pp. 1528–1538, Mar. 2016.
- [12] A. N. Vargas, L. P. Sampaio, L. Acho, L. Zhang, and J. B. R. do Val, “Optimal control of DC-DC buck converter via linear systems with inaccessible Markovian jumping modes,” *IEEE Trans. Control Syst. Technol.*, vol. 24, no. 5, pp. 1820–1827, Sep. 2016.
- [13] R. Ling, D. Maksimovic, and R. Leyva, “Second-order sliding-mode controlled synchronous buck DC–DC converter,” *IEEE Trans. Power Electron.*, vol. 31, no. 3, pp. 2539–2549, Mar. 2016.
- [14] F. L. Luo and H. Ye, *Advanced DC/DC Converters*. Boca Raton, FL, USA: CRC Press, 2016.

- [15] Y. Zhao, W. Qiao, and D. Ha, "A sliding-mode duty-ratio controller for DC/DC buck converters with constant power loads," *IEEE Trans. Ind. Appl.*, vol. 50, no. 2, pp. 1448–1458, Mar. 2014.
- [16] V. S. C. Raviraj and P. C. Sen, "Comparative study of proportional-integral, sliding mode, and fuzzy logic controllers for power converters," *IEEE Trans. Ind. Appl.*, vol. 33, no. 2, pp. 518–524, May 1997.
- [17] V. Utkin, "Sliding mode control of DC/DC converters," *J. Franklin Inst.*, vol. 350, no. 8, pp. 2146–2165, Oct. 2013.
- [18] Y. Huangfu, S. Zhuo, A. K. Rathore, E. Breaz, B. Nahid-Mobarakkeh, and F. Gao, "Super-twisting differentiator-based high order sliding mode voltage control design for DC-DC buck converters," *Energies*, vol. 9, no. 7, pp. 494–511, 2016.
- [19] S. M. RakhtAla, M. Yasoubi, and H. HosseinNia, "Design of second order sliding mode and sliding mode algorithms: A practical insight to DC-DC buck converter," *IEEE/CAA J. Automatica Sinica*, vol. 4, no. 3, pp. 483–497, Feb. 2017.
- [20] Y. Yin, J. Liu, S. Vazquez, L. Wu, and L. G. Franquelo, "Disturbance observer based second order sliding mode control for DC-DC buck converters," in *Proc. 43rd Annu. Conf. IEEE Ind. Electron. Soc.*, Oct. 2017, pp. 7117–7122.
- [21] F. Giri, O. El Maguiri, H. El Fadil, and F. Z. Chaoui, "Non-linear adaptive output feedback control of series resonant DC-DC converters," *Control Eng. Pract.*, vol. 19, no. 10, pp. 1238–1251, Oct. 2011.
- [22] Y. Cheng, H. Du, C. Yang, Z. Wang, J. Wang, and Y. He, "Fast adaptive finite-time voltage regulation control algorithm for a buck converter system," *IEEE Trans. Circuits Syst. II, Exp. Briefs*, vol. 64, no. 9, pp. 1082–1086, Sep. 2017.
- [23] S.-C. Tan, Y. M. Lai, C. K. Tse, and M. K. H. Cheung, "Adaptive feed-forward and feedback control schemes for sliding mode controlled power converters," *IEEE Trans. Power Electron.*, vol. 21, no. 1, pp. 182–192, Jan. 2006.
- [24] C. Elmas, O. Deperlioglu, and H. H. Sayan, "Adaptive fuzzy logic controller for DC-DC converters," *Expert Syst. Appl.*, vol. 36, no. 2, pp. 1540–1548, 2009.
- [25] J. Zhang, X. Liu, Y. Xia, Z. Zuo, and Y. Wang, "Disturbance observer-based integral sliding-mode control for systems with mismatched disturbances," *IEEE Trans. Ind. Electron.*, vol. 63, no. 11, pp. 7040–7048, Nov. 2016.
- [26] S. Oucheriah and L. Guo, "PWM-based adaptive sliding-mode control for boost DC-DC converters," *IEEE Trans. Ind. Electron.*, vol. 60, no. 8, pp. 3291–3294, Aug. 2013.
- [27] H. K. Khalil and J. W. Grizzle, *Nonlinear System*. Upper Saddle River, NJ, USA: Prentice-Hall, 2002.
- [28] S. Li, J. Yang, W.-H. Chen, and X. Chen, *Disturbance Observer-Based Control: Methods Application*. Boca Raton, FL, USA: CRC Press, 2016.
- [29] A. Mehta and B. Naik, *Sliding Mode Controllers for Power Electronic Converters*. Singapore: Springer, 2019.
- [30] M. Corless and G. Leitmann, "Continuous state feedback guaranteeing uniform ultimate boundedness for uncertain dynamic systems," *IEEE Trans. Autom. Control*, vol. 26, no. 5, pp. 1139–1144, Oct. 1981.



Yunfei Yin (Graduate Student Member, IEEE) received the B.S. degree in electrical engineering and automation from China Petroleum University, Dongying, China, in 2013, and the M.E. degree in control theory and control engineering from Bohai University, Jinzhou, China, in 2016. He is currently pursuing the Ph.D. degree with the Harbin Institute of Technology, Harbin, China, and with the Universidad de Sevilla (US), Seville, Spain. His current research interests include switched control, sliding mode control, adaptive control, and their applications to power electronic systems for renewable energy system.



Jianxing Liu (Senior Member, IEEE) received the B.S. degree in mechanical engineering and the M.E. degree in control science and engineering from the Harbin Institute of Technology, Harbin, China, in 2004 and 2010, respectively, and the Ph.D. degree in automation from the Technical University of Belfort-Montbéliard, Belfort, France, in 2014.

Since 2014, he has been with the Harbin Institute of Technology. His current research interests include sliding mode control, nonlinear control and observation, industrial electronics, and renewable energy solutions. He is involved in the Data Driven Control and Monitoring Technical Committee of the IEEE Industrial Electronics Society and is currently serving as an Associate Editor for the *ISA Transactions* and the *IEEE JOURNAL OF EMERGING AND SELECTED TOPICS IN INDUSTRIAL ELECTRONICS*.



Abraham Marquez (Member, IEEE) was born in Huelva, Spain, in 1985. He received the B.S., M.S., and Ph.D. degrees in telecommunications engineering from the Universidad de Sevilla (US), Seville, Spain, in 2014, 2016, and 2019, respectively. His main research interests include modulation techniques, multilevel converters, model-based predictive control of power converters and drives, renewable energy sources, and power devices lifetime extension. He was a recipient as a coauthor of the 2015 Best Paper Award of the *IEEE Industrial Electronics Magazine*.



Xinpo Lin was born in Shandong, China, in 1996. He received the B.S. degree in electrical engineering and automation from the Harbin Institute of Technology, Weihai, China, in 2017, and the M.S. degree in electrical engineering from the Harbin Institute of Technology, Harbin, China, in 2019, where he is currently pursuing the Ph.D. degree. His current research interests include sliding-mode control, neural network control, observation methods, and their applications to power electronic systems and motor driving systems.



José I. Leon (Fellow, IEEE) was born in Cadiz, Spain. He received the B.S., M.S., and Ph.D. degrees in telecommunications engineering from the Universidad de Sevilla (US), Seville, Spain, in 1999, 2001, and 2006, respectively.

Since 2019, he has been a Chair Professor with the Department of Control Science and Engineering, Harbin Institute of Technology, China. He is currently an Associate Professor with the Department of Electronic Engineering, US. His research interests include modulation and control of power converters for high-power applications and renewable energy systems. He was a co-recipient of the 2008 Best Paper Award of the *IEEE Industrial Electronics Magazine*, the 2012 Best Paper Award of the *IEEE TRANSACTIONS ON INDUSTRIAL ELECTRONICS*, and the 2015 Best Paper Award of the *IEEE Industrial Electronics Magazine*. He was a recipient of the 2014 IEEE J. David Irwin Industrial Electronics Society Early Career Award, the 2017 IEEE Bimal K. Bose Energy Systems Award, and the 2017 Manuel Losada Villasante Award for excellence in research and innovation. In 2017, he was elevated to the IEEE Fellow grade with the following citation for his contributions to high-power electronic converters.



Sergio Vazquez (Senior Member, IEEE) was born in Seville, Spain, in 1974. He received the M.S. and Ph.D. degrees in industrial engineering from the University of Seville (US) in 2006 and 2010, respectively.

Since 2002, he has been with the Power Electronics Group working in research and development projects. He is currently an Associate Professor with the Department of Electronic Engineering, USA. His research interests include power electronics systems, and modeling, modulation, and control of power

electronics converters applied to renewable energy technologies.

Dr. Vazquez was a recipient as a coauthor of the 2012 Best Paper Award of the IEEE TRANSACTIONS ON INDUSTRIAL ELECTRONICS and the 2015 Best Paper Award of the *IEEE Industrial Electronics Magazine*. He is involved in the Energy Storage Technical Committee of the IEEE Industrial Electronics Society and is currently serving as an Associate Editor for the IEEE TRANSACTIONS ON INDUSTRIAL ELECTRONICS.



Leopoldo G. Franquel (Life Fellow, IEEE) was born in Malaga, Spain. He received the M.Sc. and Ph.D. degrees in electrical engineering from the Universidad de Sevilla, Seville, Spain, in 1977 and 1980, respectively. He was an Associate Professor at the Electronics Engineering Department, Universidad de Sevilla, from 1982 to 1986, where he has been a Professor at the Electronics Engineering Department since 1986. He has also been a 1000 Talent Professor at the Department of Control Science and Engineering, Harbin Institute of Technology, since 2016.

He has participated in more than 100 industrial and research and development projects and has published more than 300 articles, 76 of them in the IEEE journals. His current research interests include modulation techniques for multilevel inverters and application to power electronic systems for renewable energy systems. He has been an IEEE Industrial Electronics Society (IES) Distinguished Lecturer since 2006. He was a Member-at-Large of the IES AdCom (2002–2003), the Vice President for Conferences (2004–2007), and the President Elect of the IES (2008–2009). He was the President of the IES (2010–2011) and is an IES AdCom Life Member. In 2009 and 2013, he received the prestigious Andalusian Research Award and the FAMA Award recognizing the excellence of his research career. He received a number of best paper awards from the IEEE journals. In 2012 and 2015, he was a recipient of the Eugene Mittelmann Outstanding Research Achievement Award and the Anthony J. Hornfeck Service Award from the IEEE-IES, respectively. In the IEEE TRANSACTIONS ON INDUSTRIAL ELECTRONICS, he became an Associate Editor in 2007, a Co-Editor-in-Chief in 2014, and the Editor-in-Chief since 2016.



Ligang Wu (Fellow, IEEE) received the B.S. degree in automation from the Harbin University of Science and Technology, China, in 2001, and the M.E. degree in navigation guidance and control and the Ph.D. degree in control theory and control engineering from the Harbin Institute of Technology, China, in 2003 and 2006, respectively. From January 2006 to April 2007, he was a Research Associate with the Department of Mechanical Engineering, The University of Hong Kong, Hong Kong. From September 2007 to June 2008, he was a Senior

Research Associate with the Department of Mathematics, City University of Hong Kong, Hong Kong. From December 2012 to December 2013, he was a Research Associate with the Department of Electrical and Electronic Engineering, Imperial College London, London, U.K. In 2008, he joined the Harbin Institute of Technology, as an Associate Professor and was then promoted to a Full Professor in 2012. He has published six research monographs and more than 150 research articles in international referred journals. His current research interests include switched systems, stochastic systems, computational and intelligent systems, sliding mode control, and advanced control techniques for power electronic systems. In 2019, he was elevated to the IEEE Fellow grade for his contributions to sliding mode control and robust filtering. He received the National Science Fund for Distinguished Young Scholars in 2015 and the China Young Five Four Medal in 2016. He was named as the Distinguished Professor of Chang Jiang Scholar in 2017 and was named as the Highly Cited Researcher from 2015 to 2019. He currently serves as an Associate Editor for a number of journals, including the IEEE TRANSACTIONS ON AUTOMATIC CONTROL, the IEEE TRANSACTIONS ON INDUSTRIAL ELECTRONICS, the IEEE/ASME TRANSACTIONS ON MECHATRONICS, INFORMATION SCIENCES, *Signal Processing*, and *IET Control Theory and Applications*. He is also an Associate Editor of the Conference Editorial Board and the IEEE Control Systems Society.